Kinetic and Mechanistic Investigations of the Formation of Polyimides under Homogeneous Conditions

Y. J. Kim, T. E. Glass, G. D. Lyle, and J. E. McGrath*

Department of Chemistry and NSF Science and Technology Center for High Performance Polymeric Adhesives and Composites, Virginia Polytechnic Institute and State University, Blacksburg, Virginia 24061-0212

Received August 25, 1992

ABSTRACT: This paper describes kinetic and mechanistic studies of the homogeneous formation of high-performance polyimides. Controlled molecular weights and nonreactive phthalimide end groups were emphasized. NMR spectroscopy, nonaqueous titration, and solution viscosity measurements were the principal techniques utilized. The disappearance of the amic acid groups was followed to quantitative conversion via nonaqueous titration with tetramethylammonium hydroxide. The homogeneous solution imidization processes were well described by auto-acid-catalyzed second-order kinetics. The effects of heteroatom electron-donating and -withdrawing bridging groups (O and SO_2) in the diamines and dianhydrides on imidization rates were investigated, and a possible reaction mechanism for the solution imidization processes was proposed. Imidization of 4,4'-oxydianiline/4,4'-oxydiphthalic anhydride poly(amic acid) was investigated at three different temperatures (140, 150, and 180 °C). Two-dimensional ^1H-^1H correlation spectroscopy and intrinsic viscosity measurements provided direct evidence for partial degradation of the poly(amic acid) backbone structures. Complete imidization, including rehealing of the broken chains, was achieved under proper reaction conditions, and the implication of these findings was considered to be very significant for the synthesis of thermally stable high-performance polyimides. For polyimide systems containing benzophenonetetracarboxylic dianhydride (BTDA), direct evidence for network formation involving imine branching and cross-linking was observed by high-field ^1H NMR spectroscopy and the formation of gels was discussed as a function of reaction conditions. One might anticipate that all ketone-containing polyimides could, to varying degrees, display this behavior.

Introduction

Aromatic polyimides are one of the most important classes of high-performance polymers. Due to their excellent electrical, thermal, and high-temperature mechanical properties, aromatic polyimides have found many applications as high-temperature insulators and dielectrics, coatings, adhesives, and matrices for high-performance composites.[1-5] Perhaps the most highly developed synthetic route for these important materials is the classical two-step method, the first step being the synthesis of poly(amic acid)s from the reaction of diamines and dianhydrides and the latter step being subsequent thermal or chemical imidization of the poly(amic acid)s.[1-10] The conversion of a poly(amic acid) to the polyimide is most commonly accomplished by thermal treatment of the poly(amic acid) in the solid state. The poly(amic acid) has usually been considered to be completely imidized after full "cure". However, there have been some questions on this point[11-14] and it is probably dependent on the heating cycle.[15,16] Thus, a final cure temperature above the glass transition temperature of the fully imidized material is needed to provide the adequate chain mobility required for a high degree of imidization. Alternatively, if a poly(amic acid) could be cyclized in solution,[17-19] relatively mild reaction temperatures could be employed, for instance 160–200 °C, which may avoid several possible side reactions that may occur at much higher temperatures, e.g., 300–400 °C. Most of the aromatic polyimides produced by the thermal solid-phase imidization process show insolubility, infusibility, and thus poor processability.[1-3] These undesirable properties that limit wider applications of the polyimides are partially due to their chain rigidity as well as to poorly defined molecular architectures such as uncontrolled molecular weight, end groups, and possibly some branches or cross-links formed during high-temperature solid-phase "curing" processes.

In our laboratory, solution imidization techniques together with molecular weight and end group control have been employed in an effort to overcome these problems.[17-26] As a result, a large number of polyimides with improved solubility and processability have been successfully synthesized, without sacrificing their many desirable properties. However, the reaction kinetics and mechanisms of thermal imidization processes, particularly a solid-phase imidization process, are clearly very complicated.[1,2,27-32] Even though a first-order kinetic equation has been almost exclusively used to treat imidization kinetic data,[1,2,33-37] the rate law of the imidization process is not well established. For example, Laius et al.[38] reported that the reaction order of the thermal imidization processes varies from 2.2 to 3.2. Lavrov et al.[39] also observed two-step second-order kinetics for the imidization of model amic acids in solution. It was also observed that carboxylic acids accelerate ring formation in the solid phase.[40] Kinetics of solid-phase imidizations have also been known to be very complex physicochemical processes,[33] being affected by many factors such as the amount of residual solvent,[27,41] film thickness,[27] molecular mobility,[38,42] physical state of the poly(amic acid),[43] conformation of macrochains,[44] and even the degree of imidization.[45] Moreover, possibilities of curing reactions other than cycloimidization were reported.[46-65] These include degradation of the poly(amic acid) backbone structures,[46-52] intermolecular imide link formation,[53,54] and network formation via possible free radical intermediates at high temperatures such as 350 °C.[55-61] Promising results on the synthesis of polyimides which had improved solubility and processability via solution imidization techniques[17-26]

* To whom correspondence should be addressed.

0024-9297/93/2226-1344$04.00/0

and the very complicated features of the solid-phase thermal imidization processes described in the literature[1-3,28-43] emphasized the need for more detailed kinetic and mechanistic studies of the formation of these very important materials in solution.

The main focus of this research was, therefore, to increase fundamental understanding of kinetic and mechanistic aspects of the imide formation reaction which is essential to the synthesis of high-performance polyimides with well-defined polymer parameters such as topology, molecular weights, and molecular weight distributions. To shed important light on the kinetics and mechanism of thermal solution imidization processes, spectroscopic methods such as two-dimensional ^1H–^1H NMR spectroscopy, quantitative nonaqueous potentiometric titration, and solution viscosity measurements were employed.

Experimental Section

Materials. High-purity 4,4′-sulfonyldibenzene-1,1′,2,2′-tetracarboxylic dianhydride (DSDA) and 4,4′-oxydiphthalic anhydride (ODPA) were obtained from Chriskev Co. and vacuum dried before using. Ultra-high-purity 3,3′,4,4′-benzophenonetetracarboxylic dianhydride (BTDA) was purchased as a white crystalline solid from Allco Chemical Co. and used after vacuum drying at 130 °C for at least 12 h. Phthalic anhydride (PA) and *tert*-butylphthalic anhydride (*t*-BuPA) purchased from Aldrich were purified by sublimation. High-purity 4,4′-oxydianiline (4,4′-ODA) purchased from Chriskev Co. was used as received. The 4,4′-diaminodiphenyl sulfone (4,4′-DDS) was obtained from Chriskev Co. and was recrystallized from deoxygenated methanol. High-purity 4,4′-isopropylidenedianiline (Bis-A) was obtained from Air Products and Chemicals, Inc., and it was used as received without further purification. The reaction solvent utilized was *N*-methylpyrrolidone (NMP), and the azeotroping agents for the solution imidization were *o*-dichlorobenzene (ODCB), *N*-cyclohexylpyrrolidone (CHP), and toluene. The amide solvents, NMP and CHP, were freshly distilled from phosphorus pentoxide, and ODCB and toluene were distilled from calcium hydride. High-purity tetramethylammonium hydroxide and potassium hydrogen phthalate were obtained from Aldrich Chemical Co. and used as received. Lithium bromide was obtained from Aldrich Chemical Co. and used after vacuum drying.

Poly(amic acid) Syntheses. Number average molecular weights of the poly(amic acid)s except those for ketimine formation reactions were controlled to a theoretical number average molecular weight ($\bar{M}_n$) of 40 000 using phthalic anhydride. For ketimine formation studies amine- or anhydride-terminated poly(amic acid)s were synthesized by using an excess amount of diamine monomer (Bis-A) or dianhydride monomer (ODPA) to upset the stoichiometry. Syntheses of poly(amic acid)s were conducted in NMP, in a nitrogen atmosphere for 12 h at 25 °C. For all of the poly(amic acid) syntheses, the dianhydride was reacted with diamine by adding it incrementally, as a solid, to the diamine solution. This monomer addition order is considered to be extremely important in the poly(amic acid) synthesis reaction because these reaction conditions may help minimize possible competing reactions such as hydrolysis of the anhydride functionality by any small amount of water which could still be present in the reaction system.[62]

One typical example of poly(amic acid) synthesis is as follows: 11.7641 g (0.058 75 mol) of 4,4′-ODA was dissolved in 149 g of dry NMP in a 500-mL four-neck round-bottom flask equipped with a mechanical stirrer, nitrogen inlet, and a drying tube. After the diamine was completely dissolved, 0.2220 g (0.001 499 1 mol) of phthalic anhydride was added to the stirring solution of the diamine and was allowed to react with the diamine for several minutes. Next, 17.9928 g of ODPA (0.0580 mol) was added as a solid incrementally to the diamine solution such that the previous addition had dissolved before more dianhydride was added. The Teflon-coated weighing dish was washed with 20 g of dry NMP. After the dianhydride addition was finished, the reaction was allowed to proceed for an additional 12 h at room temperature under nitrogen atmosphere. These conservative reaction conditions were employed to ensure that quantitative step polymerization and possible molecular weight redistribution to a most probable $\bar{M}_w/\bar{M}_n$ of 2.0 were achieved. After completion of the reaction, 73 g of NMP and 27 g of the azeotroping agent, ODCB, were added and the solution was well agitated by a mechanical stirrer. The poly(amic acid) solution was thus typically composed of 10% (w/w) solids, 81% NMP, and 9% (w/w) ODCB.

Solution Imidization of Poly(amic acid)s. Poly(amic acid)s were transformed into polyimides by utilizing now well-established thermal solution imidization techniques.[17-26] This procedure has repeatedly been found to be useful for synthesizing soluble fully imidized amorphous homo- and copolymers. The poly(amid acid)s were imidized in a 90/10 (w/w) solution of NMP/azeotroping agent at 10% (w/w) solid contents. Kinetic investigations employed ODCB as an azeotroping agent. The ^1H NMR and intrinsic viscosity studies used CHP as an azeotroping agent to investigate their behavior as a function of time. The solution imidization was carried out in a four-neck round-bottomed flask equipped with a thermocouple, a mechanical stirrer, an inversed Dean-Stark trap filled with freshly distilled ODCB, a nitrogen gas inlet, a drying tube, and a condenser. The reaction temperature was precisely controlled (±1 °C) via a thermocouple using a temperature-controllable hot plate. The amic acid solution (10% solid contents, NMP/azeotroping agent = 9/1) was introduced into the reaction flask immersed in a preheated oil bath which was 20 °C higher than the reaction temperature. This allowed the desired reaction temperature to be obtained within 10 min. In view of the time of imidization, this was considered to be an acceptable interval. Within 2 h after the imidization reaction was started, a well-separated water phase was observed in the Dean-Stark trap. The poly(amic acid) solution was allowed to imidize under a nitrogen purge at constant reaction temperatures which ranged from 130 to 180 °C. For imidization kinetics and mechanism investigations, reaction samples were withdrawn into sample vials using disposable pipets at defined time intervals, quenched using a dry ice/acetone bath, and stored in the refrigerator for future characterization.

Potentiometric Titration of Carboxylic Acid Groups. Potentiometric titrations were successfully utilized to determine the degree of imidization. Titrations of carboxylic acid functional groups of poly(amic acid) or partially imidized poly(amic acid) were performed using an MCI GT-05 (COSA Instruments Corp.) automatic potentiometric titrator. Tetramethylammonium hydroxide in methanol solution (~0.025 N) was used, and the exact concentration was determined by back-titration with potassium hydrogen phthalate. Samples for the titration were prepared by diluting 10% (w/w) polymer solution with 60 mL of dry NMP in order to require more than 4 mL of the titrant. The amount of residual amic acid (% AA) was obtained using the following equation.

$$\% \text{ AA} = \frac{\frac{M_{ru}(0)}{2} - 18}{\frac{10W}{NV} - 0.18} \quad (1)$$

where % AA = percent of residual amic acid, N = normal concentration of the titrant, V = volume of titrant consumed at the end point in milliliters, $M_{ru}(0)$ = molecular weight of a repeat unit of poly(amic acid), and W = net weight of polymer sample in grams.

Nuclear Magnetic Resonance Spectroscopy (NMR). NMR spectroscopy was used to obtain information on the microstructure of poly(amic acid) and to conduct mechanistic investigations of the solution imidization process. A Varian Unity 400 spectrometer operating at 399.952 MHz for ^1H was used to obtain the spectra. Samples analyzed could be powders, 10% polymer solutions in NMP (90%)/azeotroping agent (10%), and 10% swellable polymer gel in NMP (90%)/azeotroping agent (10%). Samples were dissolved in deuterated dimethyl sulfoxide (DMSO-d_6). In the case of the 10% swellable polyimide gel (BTDA-containing polyimide), the gel was diluted with a large excess amount of dry NMP to swell the gel and DMSO-d_6 was

added to afford a final concentration of less than 1%.

Typical conditions for ^1H spectra included the acquisition of 64 scans using a sweep width of 6500 Hz, a pulse width of 3.9 ms, an acquisition time of 3.74 s, and a recycle delay of 1.0 s. Typical conditions for the acquisition of ^{13}C spectra at 100.577 MHz included ^1H Waltz decoupling, a sweep width of 25 000 Hz, an acquisition time of 1.2 s, a pulse width of 6 ms, and a recycle delay of 1.0 s. The two-dimensional ^1H–^1H COSY spectra were recorded using the phase-sensitive COSY-90 software standard with the Varian unity. The sweep width in both dimensions was 619.8 Hz. The acquisition time in the f_2 dimension was 0.207 s. Thirty-two transients were collected for each of the 64 incremental delays in the f_1 dimension with a recycle delay between transients of 0.8 s. After zero filling once in the f_1 dimension, the resulting data matrix was 256 × 256. The Gaussian function was applied in each dimension prior to Fourier transform.

Intrinsic Viscosity Measurements. Intrinsic viscosity measurements were utilized to characterize the 4,4′-ODA/ODPA poly(amic acid) and its partially imidized product at intermediate stages. All of the intrinsic measurements were performed in anhydrous 0.1 M LiBr in NMP solution at 25 °C to minimize polyelectrolyte effects[63–65] which might occur for dilute poly(amic acid) solutions. Since polyimides with high degrees of imidization (above ca. 98% degree of imidization) may show a thermoreversible gelation phenomena, polyimide samples taken at defined time intervals were diluted with dry 0.1 M LiBr/NMP solution after quenching using a dry ice/acetone bath in order to prevent physical gelation. The gelation phenomena were a strong function of molecular weight, aging temperature, polymer concentration, moisture in the NMP, and aging time. Cannon-Ubbelohde dilution viscometers with a proper capillary size were used to determine intrinsic viscosity. The 10% (w/w) polymer solutions were prepared by dissolving in a 0.1 M LiBr in dry NMP solution. All viscosity measurements were performed at 25 °C in a temperature-controlled water bath.

Results and Discussion

Acid and Amide Signal Assignments of ^1H NMR Spectra of Poly(amic acid). ^1H NMR spectra of the poly(amic acid)s show two peaks downfield, one at around 13 ppm due to the carboxylic acid and the other at around 10.5 ppm due to the amide functional groups. Even in the literature[66,67] the acid and amide proton signal assignments have apparently been incorrect, perhaps because the acid proton signal shifts upfield in the presence of a small amount of residual water, and thus only one peak at around 10.5 ppm is observed. In this section deuterium-exchange experiments were conducted in order to unambiguously assign the acid and amide protons.

Figure 1 shows the ^1H NMR spectra of the poly(amic acid/imide) from the reaction of 4,4′-ODA/ODPA. After the imidization was completed, the two signals at 13 and 10.4 ppm completely disappeared (Figure 1E). When one drop of D_2O was added, a broad signal at 13 ppm completely disappeared (Figure 1B). On the other hand, the signal at 10.4 ppm was still present, but the intensity of the signal decreased significantly. When several drops of D_2O were added, the proton signals at 10.4 almost disappeared (Figure 1C). These experiments showed different extents of exchange between the protons of the carboxylic acid functional groups and deuterium atoms of D_2O. From these experiments the signal at 13 ppm which showed more extent of exchange was assigned to the acid proton and the signal at 10.4 ppm which showed less extent of exchange was considered to be the amide proton.

Isomeric Compositions of the 4,4′-ODA/ODPA Poly(amic acid). Since the amine functional groups can react with the anhydride functional groups by two different pathways, there are three isomeric structures in a poly(amic acid) when a triad containing two dianhydride and one diamine portion is considered. The various microstructures of the poly(amic acid) synthesized from the

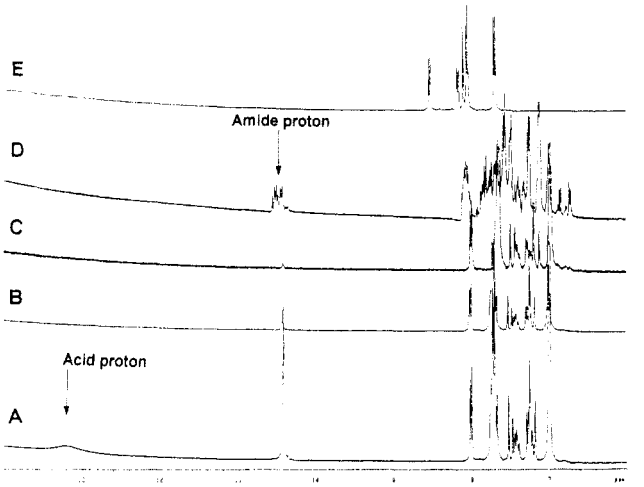

Figure 1. ^1H NMR spectra of the poly(amic acid) from the reaction of 4,4′-ODA/ODPA: (A) unreacted poly(amic acid); (B) after one drop of D_2O addition into poly(amic acid); (C) after several drops of D_2O addition into poly(amic acid); (D) partially imidized poly(amic acid); (E) completely imidized polymer.

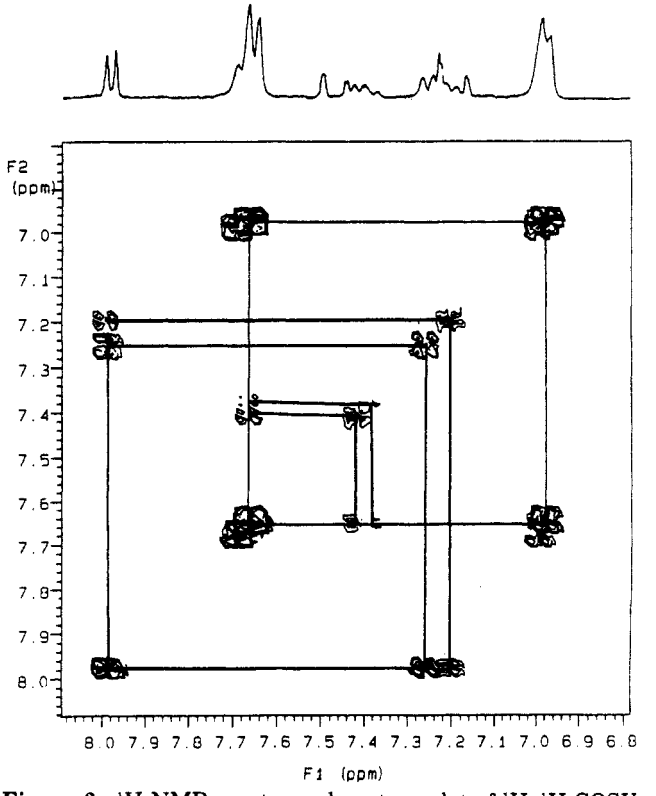

Figure 2. ^1H NMR spectra and contour plot of ^1H–^1H COSY spectra of 4,4′-ODA/ODPA poly(amic acid).

reaction of 4,4′-ODA and ODPA in NMP at room temperature were characterized by NMR spectroscopy. ^1H NMR spectra and the contour plot of ^1H–^1H COSY spectra of 4,4′-ODA/ODPA poly(amic acid) (theoretical M_n = 40K) synthesized in NMP at room temperature are shown in Figure 2. Using additivity and connectivity information obtained from the ^1H–^1H COSY spectra (Figure 2), it was possible to assign the very complicated proton spectra of 4,4′-ODA/ODPA poly(amic acid). Figure 3 shows ^1H NMR spectra with assigned chemical structures. From the signal intensity information of the ^1H NMR spectra of the poly(amic acid) (Figure 3), the microstructure of the poly(amic acid) could be obtained.

The various quantities regarding the microstructure compositions were defined as follows: $p(mm) = x$, composition of meta–meta linkages; $2p(mp) = y$, observed

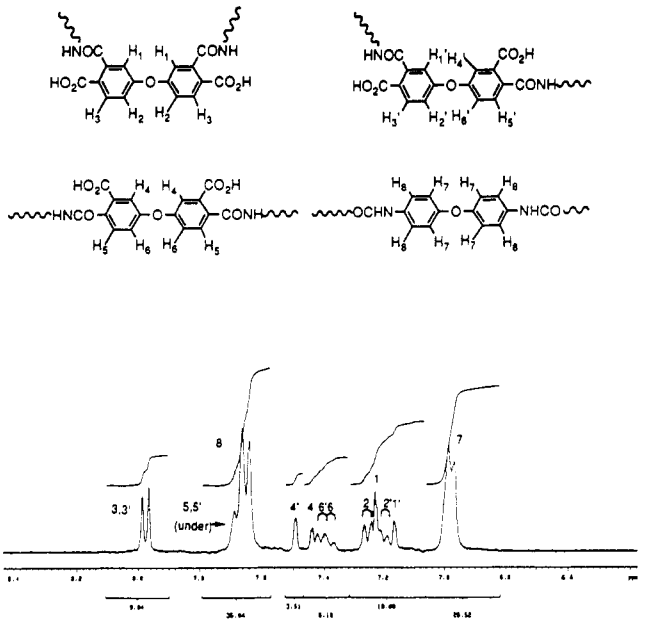

Figure 3. ^{1}H NMR spectra of 4,4′-ODA/ODPA poly(amic acid) with assigned chemical structures.

composition of meta–para linkages; $p(\mathrm{pp}) = z$, composition of para–para linkages (where p is the probability and x, y, and z are variables). Then, we have the following relationships:

$$x + y + z = 1 \tag{2}$$

$$I_3 + I_{3'} = \frac{I_t}{14}(2x + y) = 9.0 \tag{3}$$

$$I_5 + I_{5'} = \frac{I_t}{14}(2z + y) = \frac{I_t}{14}(2 - 2x - y) = 35.0 - 29.5 = 5.5 \tag{4}$$

$$I_{4'} = \frac{I_t}{14}y = 3.5 \tag{5}$$

$$I_4 + I_{6'} + I_6 = \frac{I_t}{14}(2z + y + 2z) = \frac{I_t}{14}(4 - 4x - 3y) = 8.2 \tag{6}$$

$$I_2 + I_1 + I_{2'} + I_{1'} = \frac{I_t}{14}(2x + 2x + y + y) = \frac{I_t}{14}(4x + 2y) = 19.1 \tag{7}$$

where I_i's are integrals of H_i's and I_t is the total aromatic integral (104.3).

Equation 5 gave a value of 0.47 for y, and by substitution of this value into eqs 3, 4, 6, and 7 values of x were obtained as 0.37, 0.40, 0.37, and 0.41, respectively. Internal consistency in the calculation of x values was observed with some experimental errors which confirmed the correct decoding of the ^{1}H NMR spectra of a poly(amic acid). The average of these values was 0.39. Substitution of the values x and y into eq 2 gave a value of 0.14 for z. Therefore, the poly(amic acid) prepared from 4,4′-ODA and ODPA in NMP at room temperature was composed of 0.39 meta–meta isomer $\{p(\mathrm{mm})\}$, 0.47 meta–para isomer $\{2p(\mathrm{mp})\}$, and 0.14 para–para isomer $\{p(\mathrm{pp})\}$. The microstructure information was also obtained from ^{13}C NMR spectra of 4,4′-ODA/ODPA poly(amic acid). The ^{1}H-decoupled ^{13}C NMR spectrum of 4,4-ODA/ODPA poly(amic acid) in the quaternary carbon (carbon atoms which are attached to the ether oxygen atom) region is shown in Figure 4. The

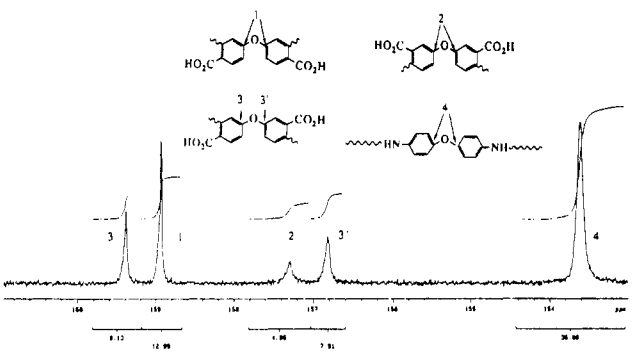

Figure 4. ^{13}C NMR spectrum of 4,4′-ODA/ODPA poly(amic acid) synthesized at room temperature in NMP.

assignment of ^{13}C NMR signals was performed by utilizing additivity information obtained from known spectra of ODPA-containing poly(amic acid).[68] Figure 4 gave microstructure compositions of 0.38 for meta–meta linkages $\{p(\mathrm{mm})\}$, 0.47 for meta–para linkages $\{p(\mathrm{mp})\}$, and 0.15 for para–para linkages $\{p(\mathrm{pp})\}$. The compositions of isomeric ratios of 4,4′-ODA/ODPA poly(amic acid) obtained from the signal intensity of ^{1}H-decoupled ^{13}C NMR spectra were similar to those obtained from ^{1}H NMR spectra, which further confirmed our correct decoding of ^{1}H NMR spectra (Figure 3).

From the higher order microstructure information, lower order information could be obtained using the following relationships:

$$p(\mathrm{m}) = p(\mathrm{mm}) + p(\mathrm{mp}) \tag{8}$$

$$p(\mathrm{p}) = p(\mathrm{pm}) + p(\mathrm{pp}) \tag{9}$$

$$p(\mathrm{mp}) = p(\mathrm{pm}) \qquad \text{reversibility rule} \tag{10}$$

When the microstructure compositions obtained from ^{13}C NMR spectra were used, the above equations gave 0.61 for the concentration of metal linkage $\{p(\mathrm{m})\}$ and 0.39 for that of para linkage $\{p(\mathrm{p})\}$. By application of a zeroth order Markovian distribution for the reaction of 4,4′-ODA and ODPA, the following relationships can be utilized:

$$p(\mathrm{mm}) = \{p(\mathrm{m})\}^2 \tag{11}$$

$$p(\mathrm{mp}) = p(\mathrm{m})p(\mathrm{p}) \tag{12}$$

$$p(\mathrm{pp}) = \{p(\mathrm{p})\}^2 \tag{13}$$

The microstructure compositions were independently obtained from eqs 11–13. Thus, the amount of meta linkages $\{p(\mathrm{m})\}$ was 0.61, and that of para linkages was 0.39. These obtained values were the same as those calculated from eqs 8–10, which implies that reactivity of anhydride groups of ODPA with amine groups of 4,4′-ODA is independent of whether neighboring groups are reacted or not. The high abundance of meta linkages also implies that the meta carbonyl groups with respect to the ether oxygen atom are more electrophilic than para carbonyl groups with respect to the ether oxygen atom under the reaction conditions.

Degree of Imidization by Potentiometric Titrations. The content of the residual acid groups of partially imidized poly(amic acid)s was required to follow imidization kinetics. FTIR spectroscopy has been proved to be a useful technique for the determination of the degree of imidization.[1,2,27,45,46] The imide bands near 1778, 1380, and 725 cm^{-1} and reference bands near 1012 and 1500 cm^{-1} are commonly used as analytical bands to follow

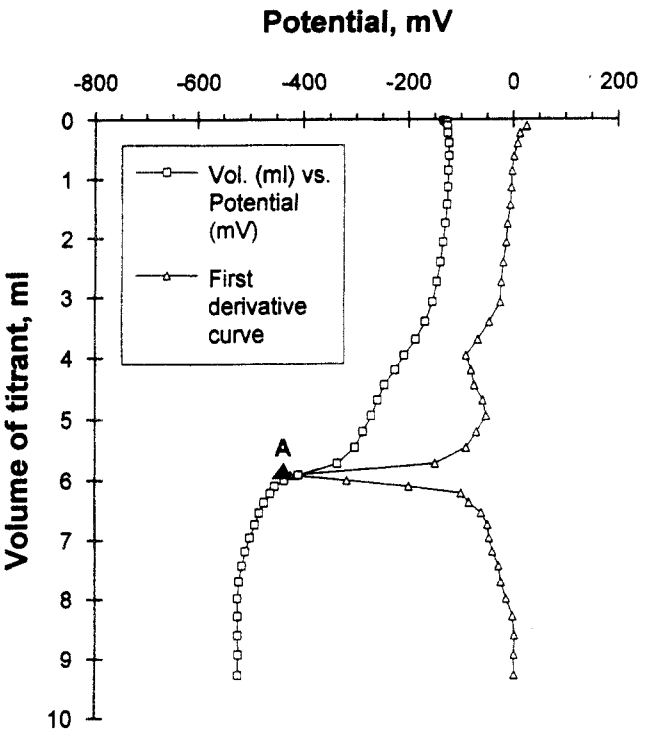

Figure 5. Titration plot for a 4,4′-ODA/ODPA polyimide system.

imidization. However, in the later stages of imidization the bands near 1778 and 725 cm^{-1} are insensitive to changes that could be detected by thermal techniques.[69] Recently, Pryde[70] has also found that the 1780-cm^{-1} band and the band near 725 cm^{-1} are affected by anhydride absorptions that appear when the polymer is heated. Clearly, this interference can result in significant errors in determining the degree of cyclization, particularly when the 1780-cm^{-1} band is used. The imide absorptions measured in film samples can also be affected by aniosotropy in the bulk imidized sample. It was also found that the average orientation of the imide groups changes as the cure proceeds.[70] Furthermore, when FTIR is used as a probe to follow imidization reactions, the observed quantitites need to be normalized to obtain the degree of imidization. Therefore, the rate constant is dependent upon the accuracy of the normalization factor. In contrast, for the titration method the rate constants could be obtained from directly measured quantities of the amount of remaining acid groups. Thus, in this research nonaqueous potentiometric titrations were advantageously utilized to obtain the degree of imidization as a function of reaction time. A weak base tetramethylammonium hydroxide was used to avoid the possible hydrolytic degradation of amide bonds of the poly(amic acid)s during the measurements.

A representative titration curve is shown in Figure 5 for the partially imidized 4,4′-ODA/ODPA poly(amic acid) for 80 min at 140 °C. Figure 5 shows a clear inflection point at the potential value of ca. −410 mV. The inflection point near the potential value of −410 mV is clearly the desired end point since the slope changes abruptly. In general, the degree of steepness of the slope near the equivalence point is dependent upon the acidity and basicity of the system to be titrated, and a steeper slope is observed for strong acid/strong base titration.[71] All of the titration plots of the partially imidized poly(amic acid/imide) investigated in this research showed clear end points at constant potential values for given systems. Once an equivalence point and thus the volume of titrant consumed at an end point (an equivalent point) were determined, the amount of residual amic acid (% AA) could be obtained using eq 1. Representative plots of reaction time (in minutes) vs the amount of unreacted acid functional groups (% AA) for various polyimide systems are also shown in Figure 6A–D.

Reaction Order of Solution Imidization Processes. Since both acid and amide functional groups belong to the same molecule, many kinetic studies have been analyzed using the first-order kinetic equation:[1,2,33-37]

$$\ln(1-p) = -kt \tag{14}$$

where p is the degree of imidization, k is a rate constant, and t is the reaction time.

Thus, we first attempted to interpret our data in this manner. The first-order kinetic plot of $-\ln(1-p)$ vs reaction time for the 4,4′-ODA/ODPA polyimide system is shown in Figure 7. The kinetic plot shows that the kinetics of imidization could apparently be described by first-order kinetics up to relatively high conversions as compared to those for the more conventional solid-phase imidization processes where deviations were observed at imidization stages as early as 30–40% conversion.[33] However, our data also showed deviations from first-order kinetics at high conversions, as observed in Figure 7. The two-step kinetic features of solid-phase imidization processes have been interpreted in terms of decreased molecular mobility,[38,42] kinetic nonequivalence,[44] and effects of solvents.[27,41,45] However, in the solution imidization processes, there is no increased T_g effect since polymers are in solution and no changes in solvent effects since the polar solvent, NMP, is in large excess throughout. Moreover, kinetically nonequivalent conformations are also expected to exchange rapidly *in solution* at elevated temperatures. Therefore deviations from first-order kinetics above 50–70% conversions in our experimental result (Figure 7) are not related to artifacts and should suggest the appropriate rate law governing these solution imidization processes. The determination of reaction order from bulk imidization kinetic data might be very difficult because (1) as mentioned earlier, imidization rates are strongly dependent upon many external variables and imidization kinetics show stepwise characteristics at low conversions (30–40%) and (2) it is also impossible to determine the reaction order by analyzing kinetic data obtained at low conversions because data for the second-order reaction are also well fitted to the first-order kinetic equation at low conversion.[72] The pertinent figure in that reference is reproduced in Figure 8.

Since the second-order kinetic data are also fitted to the first-order kinetics at low conversions, analysis of kinetic results of imidization of poly(amic acid) at low conversions cannot provide clear conclusions as to the reaction order. Thus, kinetic parameters obtained from a thermal solid-phase imidization process assuming first-order kinetics are not reliable.

With these facts in mind, concentration dependence experiments were performed to determine the reaction order of the thermal imidization processes. Solution imidization of the 4,4′-ODA/ODPA poly(amic acid)s, at sufficiently different initial concentrations, e.g., 5, 10, and 15 solids wt %, were conducted at an imidization temperature of 160 °C. As shown in Figure 9, the rate of imidization is strongly dependent upon initial concentration of the poly(amic acid) solution. If the imidization reaction followed first-order kinetics, there must, of course, be no concentration dependence on the reaction rate. Using the Noyes equation,[73] second-order kinetics were followed to very high conversions.

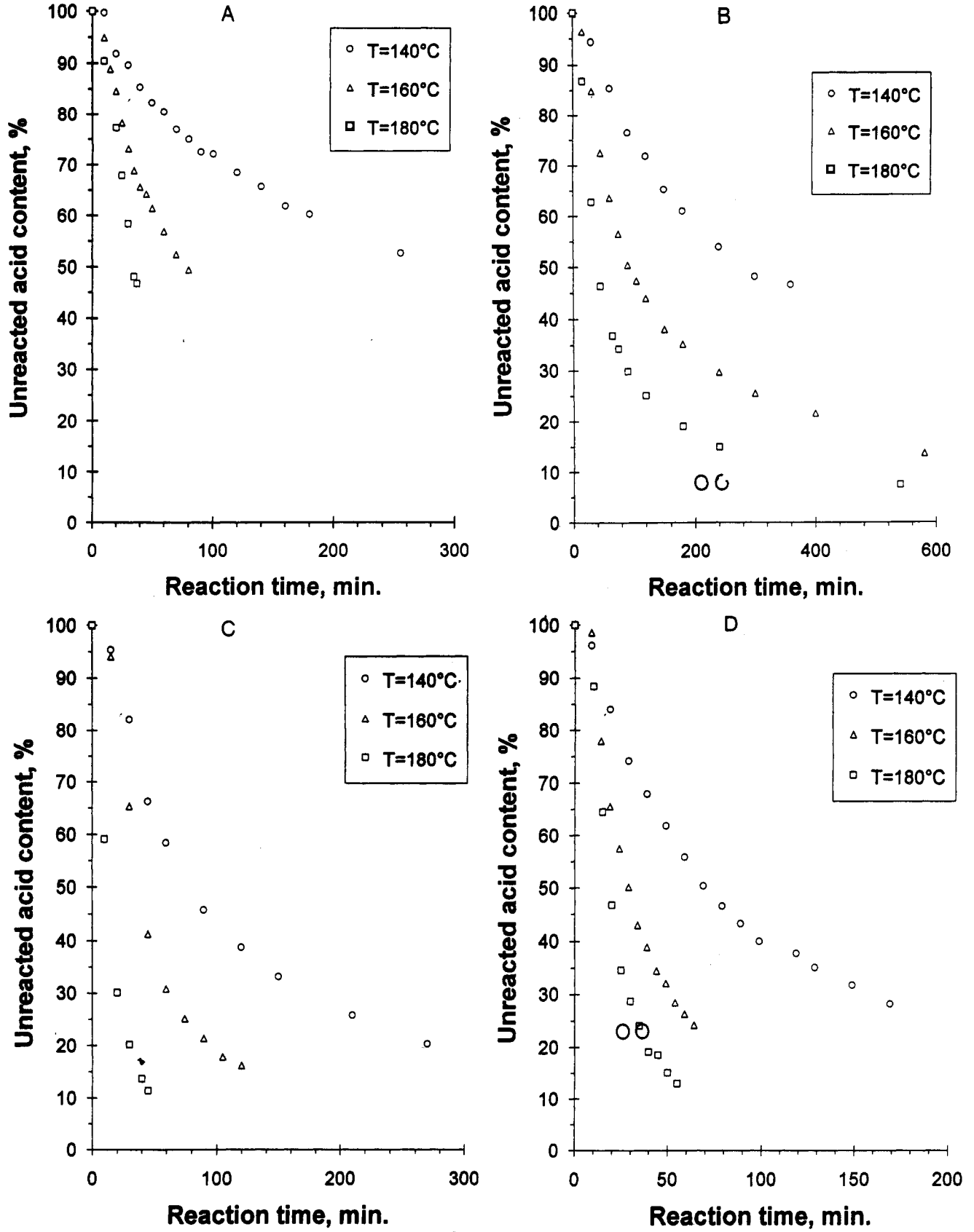

Figure 6. Plots of the amount of unreacted amic acid (%) vs reaction time for polyimide systems: (A) 4,4′-DDS/DSDA; (B) 4,4′-DDS/ODPA; (C) 4,4′-ODA/DSDA; (D) 4,4′-ODA/ODPA.

The effects of acid catalysts on the imidization kinetics were investigated, and Figure 10 shows the effects of a small amount of acid, *p*-toluenesulfonic acid, on the imidization of a 10% solution of 4,4′-ODA/ODPA poly(amic acid) at 130 °C. Acid catalysis of the imidization was clearly observed. Thus, these imidization processes are characterized by acid-catalyzed second-order reactions.

While the complex solid-phase bulk thermal imidization process has been termed as a "physicochemical process" and characterized by the two-step kinetic process, solution imidization processes have been much less studied. To our knowledge, these investigations appear to be the first demonstration that second-order kinetics are followed up to high conversions (ca. 90%). This one-step kinetic

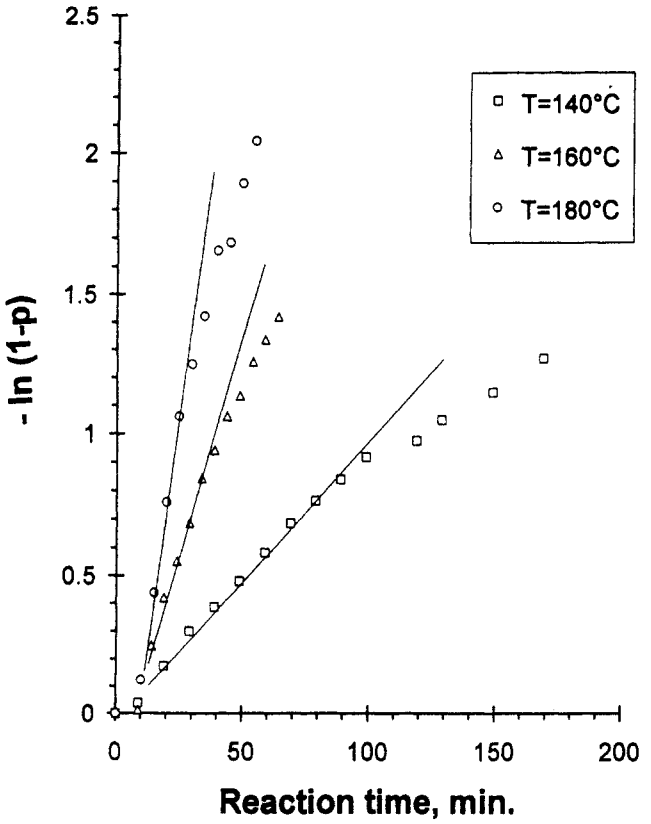

Figure 7. First-order kinetic plot of $-\ln(1-p)$ vs reaction time for 4,4'-ODA/ODPA polyimide system.

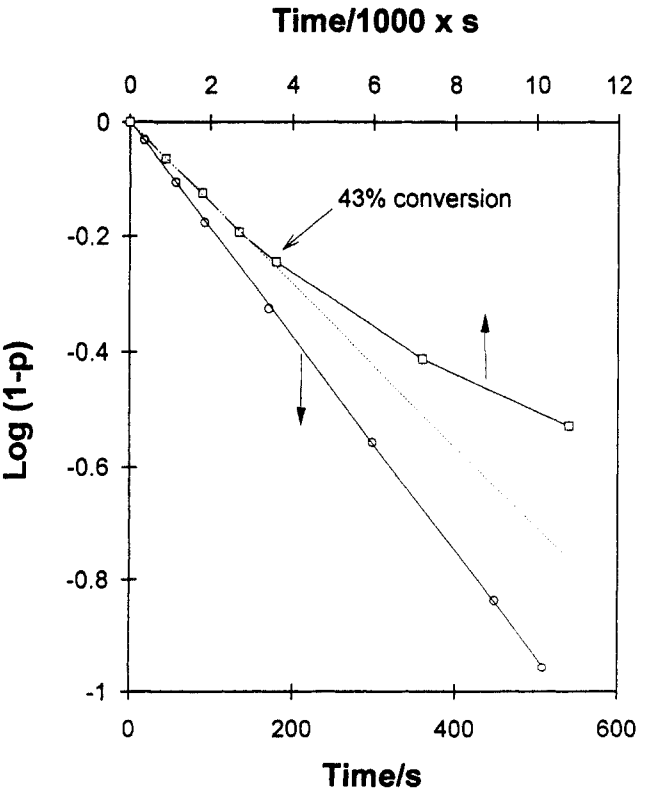

Figure 8. Kinetic data for first-order and for second-order reactions plotted as if both were first order: first order (circle); second order (square).

feature of the solution imidization processes is ascribed to the complete removal of constraints, such as a T_g rise and the existence of "kinetically nonequivalent states" of amic acid groups, that have been previously used to explain the complex, two-step kinetic features of the solid-phase imidization processes. Thus, a solution imidization process

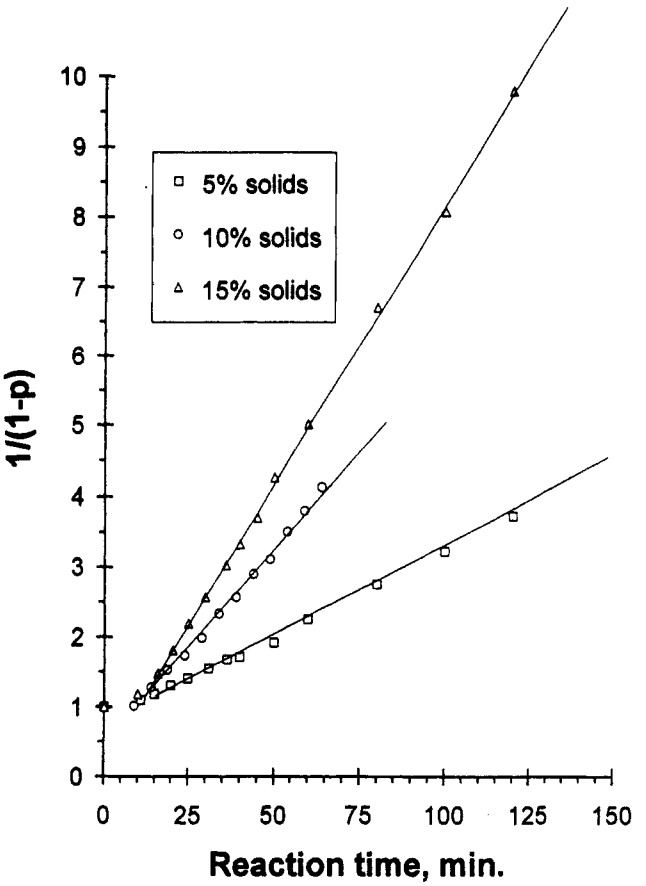

Figure 9. Demonstration of the concentration dependence of the rate of imidization for the 4,4'-ODA/ODPA polyimide system (reaction temperature = 160 °C).

could be defined as a "chemical process" where kinetics are governed by chemical reactivities of the amic acid groups.

Thus, the imidization reaction follows auto-acid-catalyzed second-order kinetics and the rate law of solution imidization processes is given by

$$-\frac{dN}{dt} = kN^2 \tag{15}$$

where N is the number of acid functional groups at time t and k is a second-order rate constant. The solution of eq 15 can be easily obtained. That is,

$$\frac{1}{N} - \frac{1}{N_0} = kt \tag{16}$$

where N_0 is the number of initial acid functional groups at $t = 0$. From eq 16 with $N = N_0(1-p)$,

$$\frac{1}{1-p} = N_0kt + 1 \tag{17}$$

In developing the above kinetic equation (eq 17) for the solution imidization processes, two basic assumptions were made to simplify the rate law. One is that the equal reactivity assumption for various amic acid groups in different chemical environments holds, and the other is that side reactions such as hydrolytic and unimolecular degradation of poly(amic acid)s have no practical effects on the kinetics of the imidization processes. To fulfill the equal reactivity assumption, monomers for kinetic investigations were deliberately selected. All of the monomers shown in Figure 11 are nonconjugated structures. Due to the nonconjugated nature of the monomers, the reactivities of the amic acid groups in the poly(amic acid)s are expected to remain practically constant in the different chemical

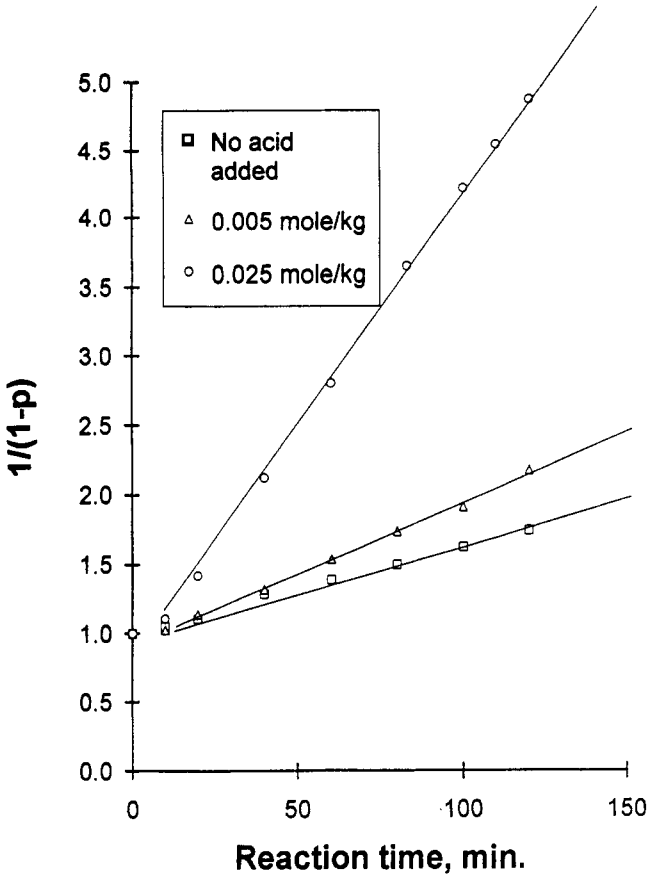

Figure 10. Acid catalysis for imidization of 4,4′-ODA/ODPA poly(amic acid)s at 130 °C, 10% solids.

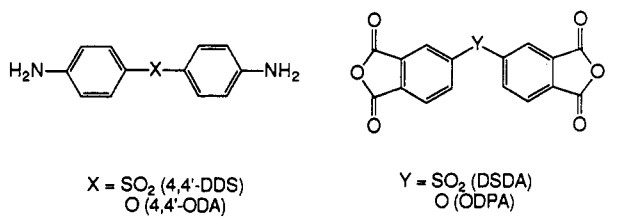

Figure 11. Diamine and dianhydride monomers for kinetic investigations.

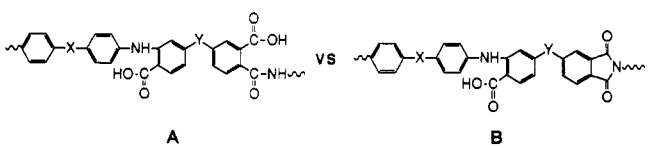

Figure 12. Amic acid groups in different chemical environments.

environments. For example, the reactivity of the amic acid groups in Figure 12A is practically the same as that in Figure 12B. The validity of this assumption could be supported by the fact that microstructure compositions of 4,4′-ODA/ODPA poly(amic acid) were observed to follow the zeroth order Markovian distribution law, as already discussed. The second assumption, whose validity is dependent upon the degree of side reactions, seems to be valid since the side reactions would only occur to a small extent, as reported elsewhere.[74,75] Moreover, the use of an azeotroping agent (*o*-dichlorobenzene) should help minimize hydrolytic degradation of the poly(amic acid)s.

Effects of Bridging Groups on the Reactivity. Second-order kinetic plots of reaction time vs $1/(1-p)$, respectively, for 4,4′-DDS/DSDA, 4,4′-DDS/ODPA, 4,4′-ODA/DSDA, and 4,4′-ODA/ODPA are shown in Figure 13. All of the kinetic data were well fitted to the second-order kinetic equation up to high conversion, except 4,4′-DDS/DSDA and 4,4′-ODA/DSDA polyimide systems. Due to the rigid characteristics of the DSDA monomer, those two polymer systems precipitated during the imidization procedures. Rate constants could be obtained from the slope of the second order kinetic plots of reaction time vs $1/(1-p)$.

The temperature dependence of the rate constants could be expressed by the Arrhenius relation (eq 18) which employs frequency factor (A) and activation energy (E_a) or the absolute rate theory relation (eq 19) which employs two adjustable parameters, activation enthalpy ($\Delta H^{\ddagger}$) and activation entropy ($\Delta S^{\ddagger}$). In eq 19 κ is a transmission

$$k = A \exp\left(-\frac{E_a}{RT}\right) \tag{18}$$

$$k = \kappa \frac{RT}{Lh} \exp\left(\frac{\Delta S^{\ddagger}}{R}\right) \exp\left(-\frac{\Delta H^{\ddagger}}{RT}\right) \tag{19}$$

coefficient which is usually taken as unity, L is the Avogadro constant, and h is the Plank constant. On the basis of these two equations (eqs 18 and 19) and rate constants, kinetic parameters were obtained. The Arrhenius plot and the derived kinetic parameters are shown in Figure 14 and Table I, respectively. The kinetic results in Table I demonstrate that the rate of the imidization reaction is influenced by the heteroatom bridging groups in both diamine and dianhydride components. In the temperature range examined, the reactivity order for the imidization is 4,4′-ODA/DSDA ≥ 4,4′-ODA/ODPA ≫ 4,4′-DDS/DSDA ≥ 4,4′-DDS/ODPA polyimide system. Obviously, an electron-donating group (–O–) in the diamine component accelerates the rate of imidization significantly due to direct electronic effects on the amide nitrogen atom. The rates of imidization for the 4,4′-ODA/ODPA polyimide system containing an electron-donating group in the dianhydride component were observed to be comparable to those of the 4,4′-ODA/DSDA polyimide system containing a strong electron-withdrawing group in the dianhydride component at low temperatures, 140 and 160 °C. Moreover, the rates of imidization for the 4,4′-DDS/ODPA polyimide were also comparable to those of the 4,4′-DDS/DSDA polyimide system at low temperatures. In addition, polyimide systems containing DSDA showed slightly increased imidization rates at 180 °C. Thus, the effects of the bridging groups of dianhydride components on the reactivity were relatively small. One may speculate on this behavior as follows; Figure 15 shows one of the repeat units in the poly(amic acid). A bridge group X in the diamine component can exert a direct electronic effect on the amide nitrogen atom which is in the para position with respect to X via resonance. On the other hand, the Y group in the dianhydride component may exert electronic effects on both the amide nitrogen and acid carbonyl groups. For example, if Y is an electron-donating group such as oxygen, it will decrease the electrophilicity of the para acid carbonyl group (A in Figure 15) via resonance. At the same time the oxygen atom would increase the electron density of the para amide carbonyl group (B in Figure 15). Thus, the nucleophilicity of the amide nitrogen (B in Figure 15) would be increased. But the Y group would exert more electronic effects on the para acid carbonyl groups than on the para amide nitrogen groups. As a result, electronic effects of bridging groups in the dianhydride component are not as significant as those of diamine components.

For intramolecular reactions, it was suggested that optimum orientations of the reactive functional groups are required to allow adequate interactions between those

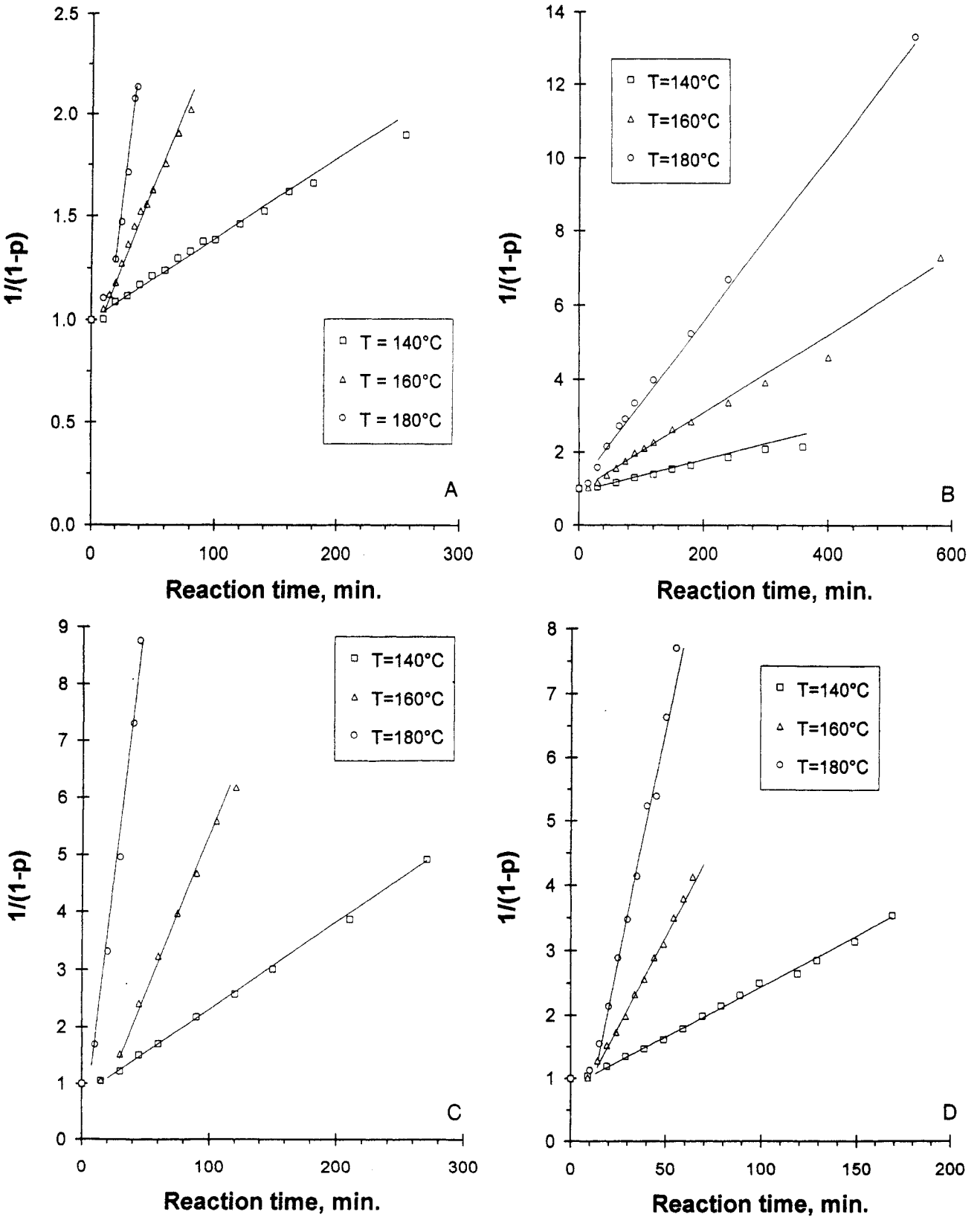

Figure 13. Second-order kinetic plot of $1/(1-p)$ vs reaction time for (A) 4,4′-DDS/DSDA, (B) 4,4′-DDS/ODPA, (C) 4,4′-ODA/DSDA, and (D) 4,4′-ODA/ODPA polyimide systems.

functional groups.[76-79] Due to this reason, it was considered that chain stiffness also plays an important role in the intramolecular reactions. If this argument is true, the rigid DSDA component might have a tendency to reduce the rate of imidization. In this case, the stiffness of the dianhydride components would have a more significant influence on the reactivity than the diamine components, because both the carboxylic acid groups and amide groups are derived from the dianhydride monomer.

The activation parameters shown in Table I are not easily explained, but the slow reaction rate for the 4,4′-DDS/ODPA polyimide system is suggested to be primarily due to a relatively large negative activation entropy. However, it is important to note that the numerical values of preexponential factors such as the activation entropy ($\Delta S^{\ddagger}$) and Arrhenius frequency factor (A) vary with the choice of concentration units, except for first-order reactions.[80]

Table I
Kinetic Parameters Derived from Second-Order Kinetics for Various Polyimide Systems[a]

polyimide systems	k [g/(mol min)] 140 °C	160 °C	180 °C	E_a (kJ/mol)	ln(A) (min)	ΔH^* (kJ/mol)	ΔS^* [J/(mol K)]
4,4′-DDS/DSDA	12 ± 1	43 ± 1	160 ± 20	100 ± 3	31.6	97 ± 3	−28
4,4′-DDS/ODPA	11 ± 1	32 ± 1	70 ± 3	74 ± 5	23.9	70 ± 5	−92
4,4′-ODA/DSDA	41 ± 1	144 ± 3	560 ± 40	101 ± 5	33.2	97 ± 5	−15
4,4′-ODA/ODPA	39 ± 1	144 ± 3	380 ± 20	89 ± 5	29.5	85 ± 5	−45

[a] Where k is a rate constant, E_a is an activation energy, A is the Arrhenius frequency factor, ΔH^* is the activation enthalpy, and ΔS^* is the activation entropy.

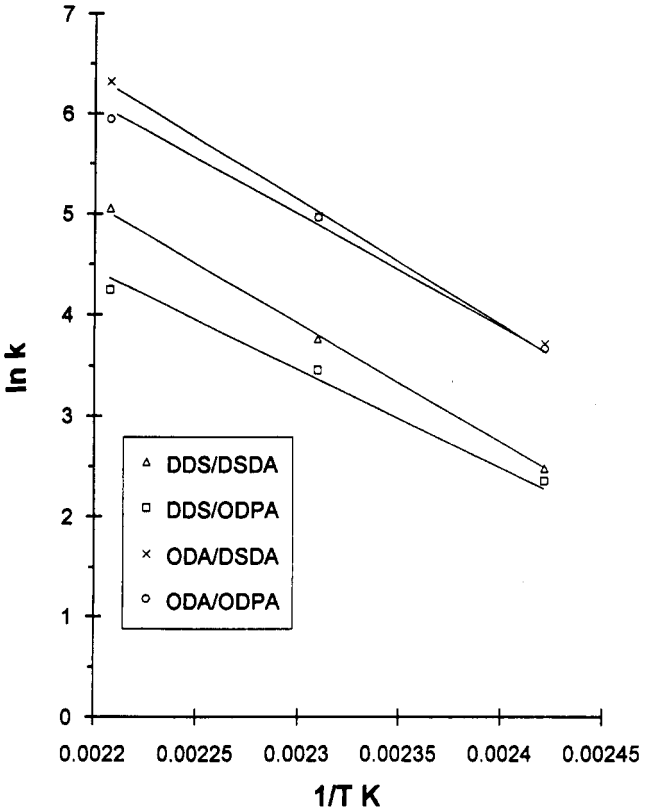

Figure 14. Arrhenius plot of second-order kinetic data for polyimide systems.

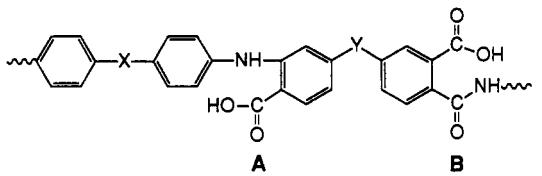

Figure 15. Representative repeat unit of a poly(amic acid).

Proposed Mechanism for the Solution Imidization Processes. On the basis of the obtained kinetic data, we propose what we believe to be a reasonable imidization mechanism, shown in Figure 16. In fact, mechanisms for the imidization reactions involving a partial prior dissociation of carboxylic acid functional groups may not be excluded. In this case, however, information on proton-transfer steps is needed. The reaction mechanism shown in Figure 16 emphasizes a bimolecular, concerted mechanistic feature. On the basis of the effects of diamine components on the reactivity, the first step should be a rate-determining step (rds). The reaction mechanism generates second-order kinetics and is also consistent with the observed acid catalysis.

NMR Studies of the Solution Imidization Processes. Figure 17 shows the ^{1}H NMR spectra of a 4,4′-ODA/ODPA poly(amic acid/imide) at intermediate conversion stages at an imidization temperature of 150 °C. As

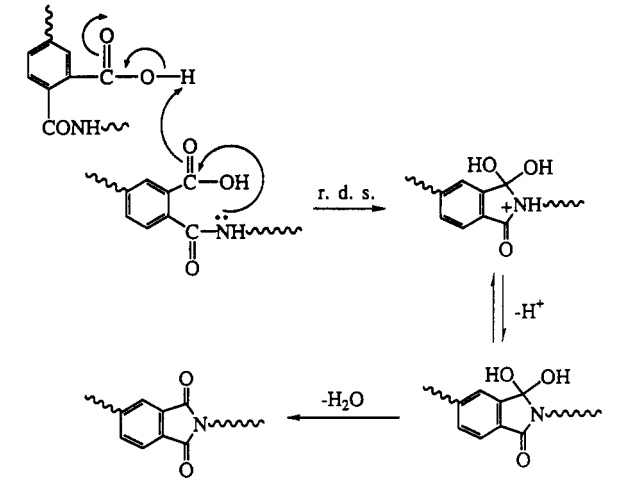

Figure 16. Possible reaction mechanism for the solution imidization process.

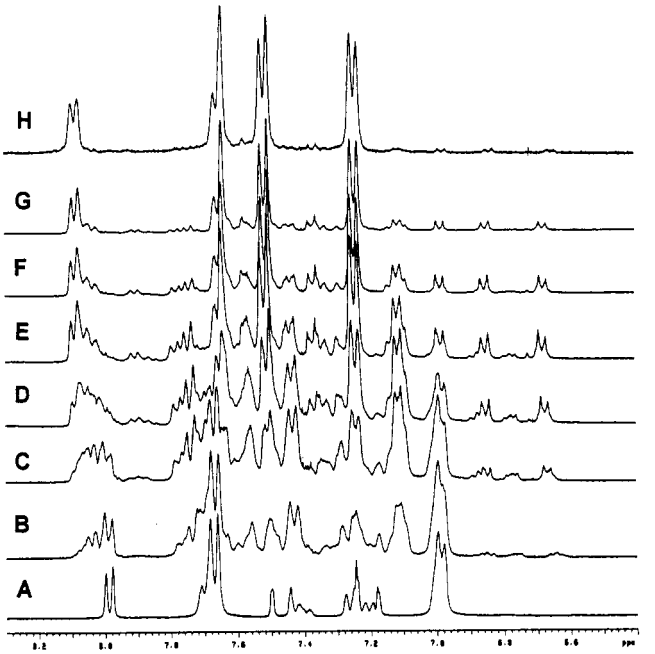

Figure 17. ^{1}H NMR spectra of 4,4′-ODA/ODPA poly(amic acid/imide) at different imidization stages imidized at 150 °C: (A) 0 h (poly(amic acid)); (B) 0.33 h; (C) 0.5 h; (D) 0.88 h; (E) 1.33 h; (F) 2 h; (G) 4 h; (H) 21 h.

imidization proceeded, the characteristic amic acid peaks originally present decreased in intensity and new peaks developed. This was especially true in the 6.6–6.9 ppm region, where upfield-shifted small peaks developed at the very beginning of imidization, increased, and then decreased in intensity as imidization proceeded.

From the ^{1}H–^{1}H COSY spectra of partially cured 4,4′-ODA/ODPA polyimide shown in Figure 18 the ^{1}H–^{1}H connectivity between the 6.67 and 6.85 ppm peaks was observed. Using this connectivity and the upfield-shifted nature of these peaks, it was possible to assign these to

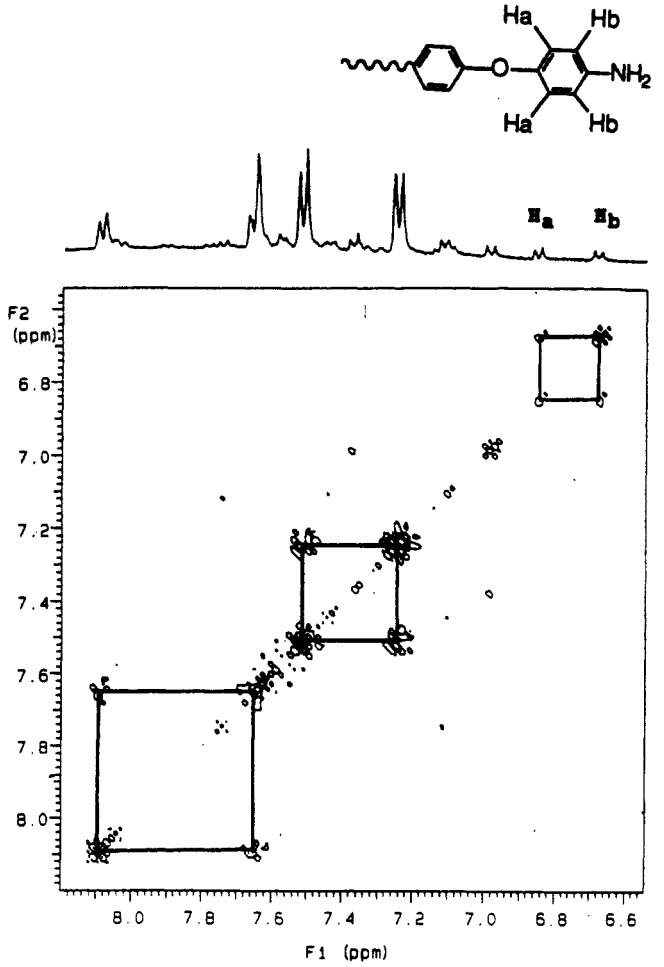

Figure 18. ^1H–^1H COSY spectra of partially imidized 4,4′-ODA/ODPA polyimide (3 h, at 150 °C).

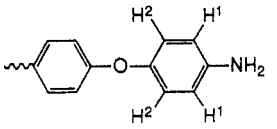

δ_{H1} = 6.67 ppm, δ_{H2} = 6.85 ppm, $J_{1,2}$ = 8.2 Hz

Figure 19. Chemical structure of the end group as a result of degradation of polymer backbone structures.

protons of the terminal amino aromatic moieities (Figure 19).

This result is clear and direct evidence of the partial degradation of the amide bonds in the polymer backbone during the imidization processes. This behavior is consistent with many earlier observations that poly(amic acid)s undergo chain cleavage, or at least viscosity reduction during thermal imidization.[46-52] The chain cleavage might be postulated to be due to a shift in the equilibrium of the amine–anhydride/amic acid system toward the direction of the amine–anhydride, and/or to a simple acid-catalyzed hydrolysis of amide bonds in the polymer backbone. However, it is not simple to resolve those two possibilities.

Molecular Weight (Intrinsic Viscosity) Changes during the Solution Imidization Processes. Parts A–C of Figure 20 show intrinsic viscosity data as a function of reaction time at 140, 150, and 180 °C, respectively. A dramatic decrease in intrinsic viscosity at the initial stages of imidization was observed. Further imidization gave rise to an increase in viscosity. Since molecular structure

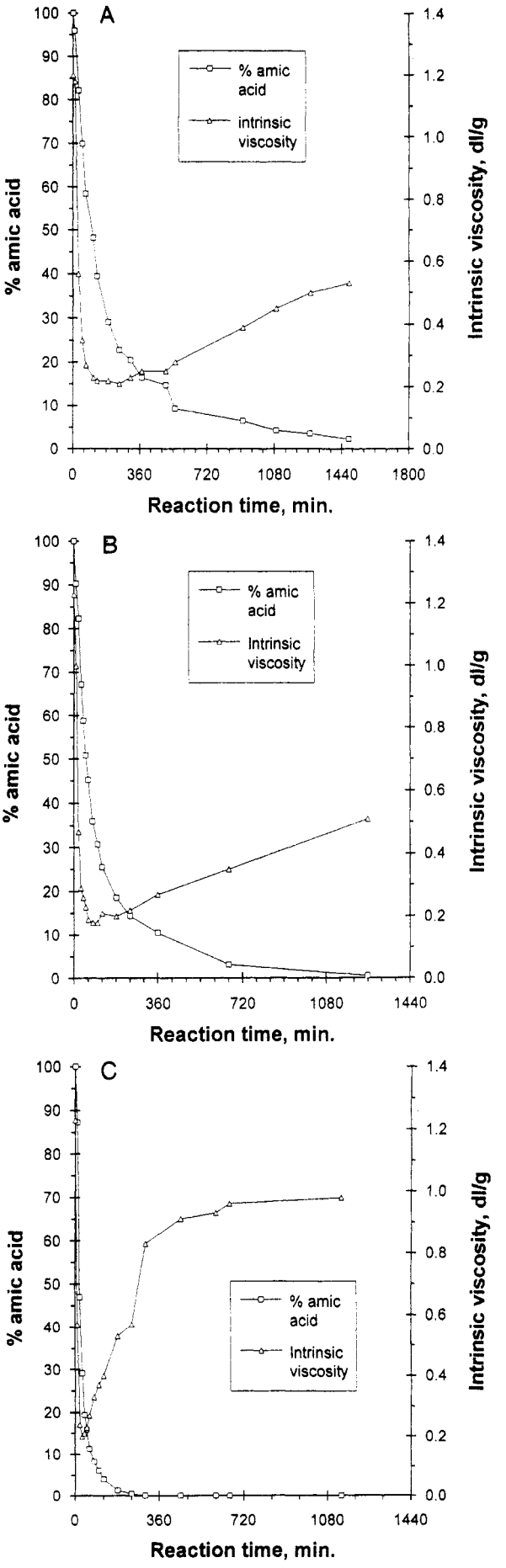

Figure 20. Remaining amic acid content and intrinsic viscosity as a function of reaction time: (A) at 140 °C; (B) at 150 °C; (C) at 180 °C.

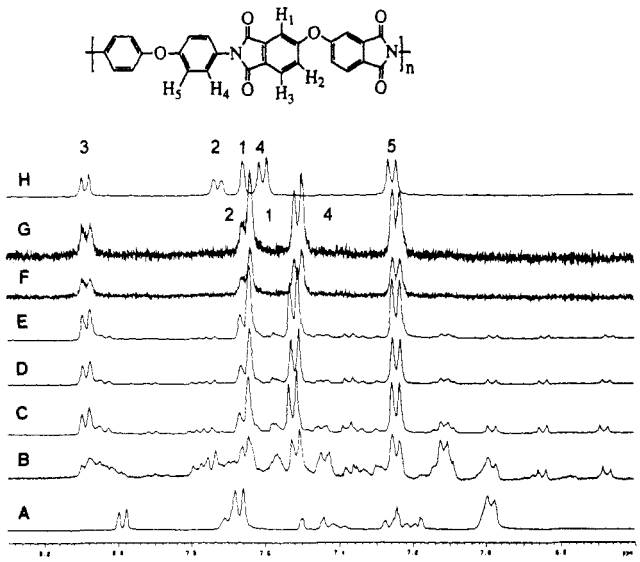

Figure 21. ^{1}H NMR spectra of 4,4′-ODA/ODPA poly(amic acid/imide) at different imidization stages imidized at 180 °C: (A) 0 h (poly(amic acid)); (B) 0.33 h; (C) 0.66 h; (D) 1 h; (E) 1.66 h; (F) 3 h; (G) 11 h; (H) 11 h (diluted with dry NMP).

changes (e.g., amic acid to imide) are occuring, a direct estimate of $\bar{M}_n$ is not possible. However, a noticeable temperature effect on the solution viscosity was observed. At relatively low imidization temperatures (140 and 150 °C) intrinsic viscosity increased very slowly and it is proposed that the degraded chain end products did not completely recombine. This is shown in Figure 17H where a sample imidized for 21 h still showed signals due to terminal amino aromatic moieties at 6.67 and 6.85 ppm, even though their intensities were small. The presence of those signals is an indication of incomplete "relinking" of the hydrolytically and/or unimolecularly decomposed chains at 150 °C. However, at higher imidization temperature (180 °C), intrinsic viscosity values rapidly increased to reasonably high values and then gradually increased to the limiting value. We suggest that the rate-controlling step for the "rehealing" is the generation of anhydride bonds from the ortho dicarboxylic acid ends.

Figure 21 shows ^{1}H NMR spectra of poly(amic acid/imide) which was imidized at 180 °C as a function of imidization time. Since completely imidized 4,4′-ODA/ODPA polyimide was insoluble in DMSO (dimethyl sulfoxide), dry NMP was added to dissolve the polyimide for NMR characterization. When polyimide samples were diluted with dry NMP, aromatic protons in the range 7.5–7.6 ppm were well resolved and even a chemical shift change was observed, as shown in Figure 21H. *Complete imidization, in terms of relinking of the partially degraded products and further cyclization of the reproduced amic acid, was possible at 180 °C.* Thus, Figure 21H shows complete disappearance of 6.67 and 6.85 ppm signals of the end groups and is entirely consistent with a complete relinking reaction. The implication of these findings is significant for the high-performance polyimide synthesis since it demonstrates that proper imidazation conditions are required to ensure complete recombination of the broken chains and their subsequent cycloimidization. Implicitly, this would also be necessary to achieve successful molecular weight control and to maximize thermal and hydrolytic stability. In our laboratory, polyimides with controlled molecular weights and nonreactive end groups have been synthesized utilizing phthalic anhydride to improve solubility and processability. For the purpose of estimating the number average molecular weight ($\bar{M}_n$), *tert*-butylphthalic anhydride was used, since it can contribute 18 unique terminal aliphatic protons. The ^{1}H NMR spectra of a 15K 4,4′-ODA/ODPA poly(amic acid) and polyimide are shown in Figure 22. The poly(amic acid) (10% solid contents, NMP/ODCB = 9/1) was imidized at 180 °C for 11 h. The ^{1}H NMR spectrum of the poly(amic acid) shown in Figure 22A suggests successful molecular weight control of the poly(amic acid) since the spectrum does not show amino aromatic end group signals in the range 6.6–6.9 ppm. Figure 22B further demonstrates complete imidization of the poly(amic acid). Investigations of $\bar{M}_w$ by light scattering measurements is consistent with these results.[23]

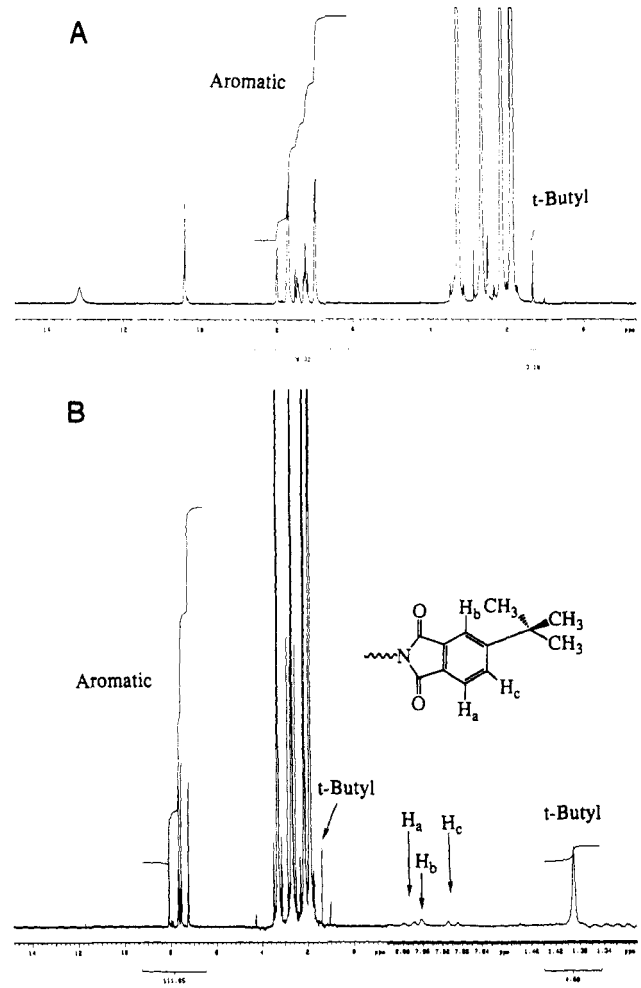

Figure 22. ^{1}H NMR spectra from the imidization of 15K 4,4′-ODA/ODPA poly(amic acid): (A) poly(amic acid); (B) fully cyclized polyimide after 11-h reaction at 180 °C.

Ketimine Formation during Solution Imidization Processes. The imine formation reaction between a carbonyl group and a primary amine is one of the classical reactions of organic chemistry. In our laboratory, the imine formation reaction has been utilized for the synthesis of semicrystalline poly(arylene ethers)[81] and poly(arylene sulfides)[82] via amorphous ketimine precursors. For benzophenonetetracarboxylic dianhydride (BTDA) containing polyimide systems, gelation due to ketimine formation was observed during imidization of the poly(amic acid)s under certain imidization conditions. However, the formed gels were easily hydrolyzed at room temperature by addition of a catalytic amount of aqueous hydrochloric acid, which is one of the characteristic features of ketimine compounds. Any residual amount of this structural imperfection would constitute a long-chain branch, which would influence melt viscosity and processing. Direct evidence of the ketimine formation reaction during thermal imidization processes was obtained from ^{1}H NMR spec-

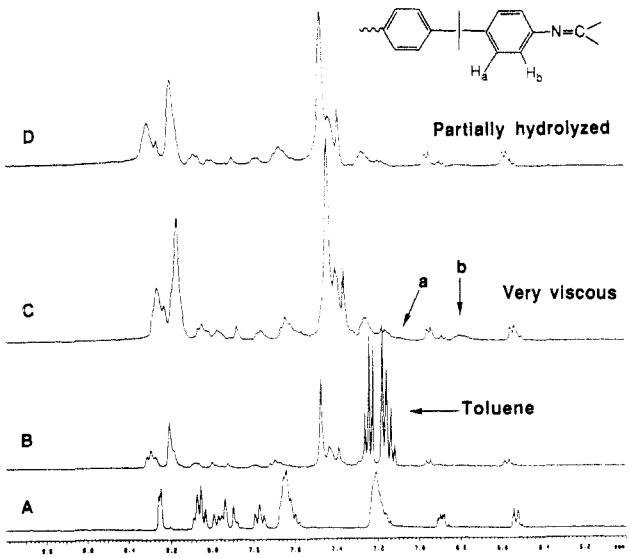

Figure 23. ^{1}H NMR spectra from the imidization of amine-terminated 3.5K Bis-A/BTDA poly(amic acid) at 130 °C: (A) poly(amic acid); (B) 8-h imidization; (C) 8.67-h imidization. (D) Polymer sample whose ^{1}H NMR spectra is shown in (C) was hydrolyzed for 3 days without acid catalysis.

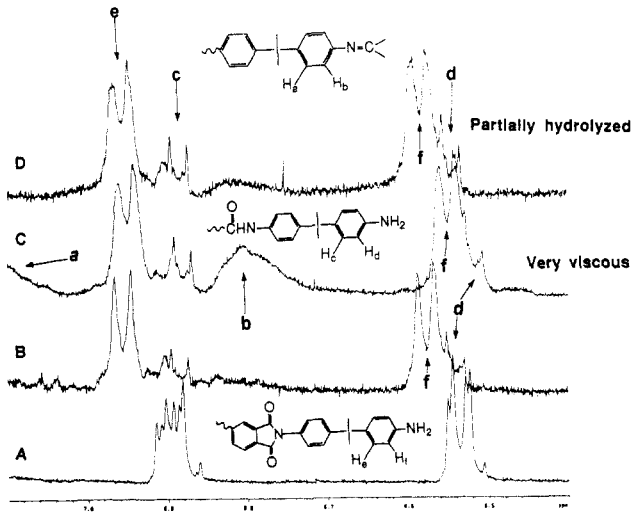

Figure 24. Expended ^{1}H NMR spectra of the ^{1}H NMR spectra shown in Figure 23 in the range 6.4–7.1 ppm.

troscopy. Figures 23 and 24 show the ^{1}H NMR spectra from the imidization of amine-terminated 3.5K Bis-A/BTDA poly(amic acid) as a function of reaction time. The imidization of the amine-terminated poly(amic acid) (10% solids) was carried out at 130 °C in NMP (9)/toluene (1) solution. Using the Dean-Stark trap containing dry toluene, the azeotroping agent (toluene) was continuously refluxed during the imidization reaction. The two peaks at 6.53 and 6.89 ppm in the bottom spectrum (Figure 24A) are due to the aminophenyl end groups, providing existence of amine-terminated end groups. After an 8-h reaction, spectrum B (Figure 24) was obtained. At this stage, no solution viscosity change was noted. For the next 40 min the toluene was stripped off from the reaction flask, and within 40 min the polymer solution formed a gel. The gel was found to be easily hydrolyzed within a few minutes by addition of aqueous hydrochloric acid, and it was also possible to be hydrolyzed at room temperature without added acids. After addition of a small amount of water, hydrolysis was allowed to proceed for 3 days. After 3 days, a significant solution viscosity drop was noted and the peaks at 6.8 and 7.1 ppm had almost disappeared. Thus, the peaks at 6.8 and 7.1 ppm are assigned to ketimine-containing aromatic protons, as shown in spectrum D (in Figure 24).

Table II
Gelation Behavior of Amine-Terminated BTDA/Bis-A Polyimides

end groups	$\langle M_n \rangle^b$	rxn temp (°C)	solvents[c]	gelation[d]
amines	80K	180	NMP (9)/ODCB (1)	yes
amines	10K	180	NMP (9)/CHP (1)	no
amines	5K	180	NMP (9)/ODCB (1)	no
amines	5K	130	NMP (9)/Tol (1)	yes
amines[a]	3.5K	130	NMP (8.5)/Tol (1.5)	yes
anhydrides	5K	180	NMP (9)/ODCB (1)	no

[a] After 8-h imidization, toluene was stripped off from the reaction flask. [b] Theoretical number average molecular weight via Carothers equation. [c] NMP = *N*-methylpyrrolidone. ODCB = *o*-dichlorobenzene CHP = *N*-cyclohexylpyrrolidone. Tol = toluene. [d] Yes: gelation occurred within 24-h reaction. No: gelation did not occur within 24-h reaction.

Table II shows the results of a gelation study of amine-terminated BTDA/Bis-A polyimide systems. As shown in Table II, it was found that extremely dry reaction conditions and low reaction temperatures favored imine formation reactions. The fact that gelation was observed only for the high molecular weight 80K system when imidized at 180 °C suggests that ketimine formation reaction during imidization processes is a nonquantitative reaction. Thus, even a small extent of ketimine reaction could cause gelation for large macromolecules (80K). The requirement of the extremely dry reaction conditions for the imine formation reaction was a quite natural result, since the imine functional group is hydrolytically unstable and the removal of water drives the reaction in the direction of imine formation. The temperature dependence of the imine formation reaction is not clearly understood at this point, but one plausible explanation is acid catalysis of the imine formation reaction. It is known that ketimine formation is favored at an intermediate pH (3–5) because the acid has effects on both the nucleophilicity of amine functional groups and the electrophilicity of carbonyl groups.[83,84] From our studies of imidization kinetics it is obvious that the rate of imidization at 180 °C is significantly different from that conducted at 130 °C. Thus, at 180 °C the imidization was so fast that acidity of the medium was not appropriate for ketimine formation; however, at low temperature (130 °C) perhaps the optimum pH of the system was achieved due to the relatively slow imidization rate.

Conclusions

Detailed, fundamental kinetic and mechanistic studies of the formation of high-performance, fully cyclized polyimides under homogeneous conditions were performed using NMR spectroscopy, nonaqueous titrations, and intrinsic viscosity measurements. For the solution imidization processes, second-order kinetics were clearly demonstrated, especially from the concentration dependence experiments, and the imidization reaction was shown to be acid catalyzed. While the solid-phase bulk thermal imidization process has been known as a physicochemical process and characterized by the two-step kinetic process, the solution imidization processes have been much less studied, even though they are conceptually more straightforward. This research appears to be the first demonstration that second-order kinetics are followed up to high conversions (ca. 90%). This one-step solution imidization process is ascribed to the complete removal of constraints, such as a T_g rise and the existence of kinetically

nonequivalent states of amic acid groups, that have been used to explain the complex kinetic features of the solid-phase imidization processes. Thus, a solution imidization process could be defined as a chemical process where the kinetics are governed by the chemical reactivities of the amic acid groups. Heteroatom functional groups in the diamine and dianhydride components influence the imidization kinetics. An electron-donating group in the diamine component accelerated the rate of imidization very significantly, but somewhat surprisingly, the effects of the dianhydride components of the rate of imidization were relatively small, as compared to those of diamine components. On the basis of these results, a concerted imidization mechanism was proposed.

Two-dimensional ^1H–^1H correlation spectroscopy (^1H–^1H) COSY) clearly demonstrated the partial degradation of amide bonds during the NMP/CHP solution imidization of poly(amic acid)s synthesized from 4,4′-oxydianiline and oxydiphthalic anhydride. At the very initial stages of the imidization process, the molecular weight (intrinsic viscosity) of the materials was observed to be dramatically decreased by just minor amounts of degradation. Subsequently, the molecular weight increased as the "recombination" of the broken chains proceeded upon further imidization. Nevertheless, complete recombination and cycloimidization, as evidenced by well-defined ^1H NMR spectra, were possible under proper reaction conditions. The implication of these findings is significant for high-performance polyimide synthesis since it demonstrates that proper imidization conditions are required to ensure complete recombination of the broken chains and their subsequent cycloimidization. Implicitly, this would also be necessary to achieve successful molecular weight control and to maximize thermal and hydrolytic stability.

Imidization of poly(amic acid)s derived from ketone-containing BTDA and Bis-A was also investigated by utilizing ^1H NMR spectroscopy. This appears to be the first direct spectroscopic data for imine linkage formation during a thermal imidization process. Extremely dry reaction conditions and relatively low reaction temperatures, e.g., 130 °C, favored imine formation reactions.

Acknowledgment. The authors greatly appreciate the support of this research by the NSF Science and Technology Center for High Performance Polymeric Adhesives and Composites under Contract DMR-912004.

References and Notes

(1) Mittal, K. L., Ed. *Polyimides: Synthesis, Characterization and Applications*, Plenum: New York, 1984, Vols. 1 & 2.
(2) Feger, C. J., Khojasteh, M. M.; McGrath, J. E., Eds. *Polyimides: Materials, Chemistry and Characterization*, Elsevier Science Publishers B.V.: Amsterdam, 1989.
(3) Wilson, D., Stenzenberger, H. D., Hergenrother, P. M., Eds. *Polyimides*; Blackie & Son Ltd.: Glasgow and London, 1990.
(4) Lupinski, J. H., Moore, R. S., Eds. *Polymeric Materials for Electronics Packaging and Interconnection*; ACS Symposium Series 407; American Chemical Society: Washington, DC, 1989.
(5) Takekoshi, T. *Adv. Polym. Sci.* **1990**, *94*, 1.
(6) Cassidy, P. C.; Fawcett, N. C. In *Encyclopedia of Chemical Technology*; Grayson, M., Ed.; Wiley: New York, 1982; Vol. 18, pp 704–719.
(7) Verbicky, J. W., Jr. In *Encyclopedia of Polymer Science and Engineering*, 2nd ed.; Mark, H. F., Bikales, N. M., Overberger, C. G., Menges, G., Eds.: Wiley: New York, 1988; Vol. 12, pp 364–383.
(8) Harris, F. W. in *Polyimides*; Wilson, D., Stenzenberger, H. D., Hergenrother, P. M., Eds.; Blackie & Son Ltd.: Glasgow and London, 1990; Chapter 1.
(9) Sroog, C. E. *J. Polym. Sci. Macromol. Rev.* **1976**, *11*, 161.
(10) Sroog, C. E. *Prog. Polym. Sci.* **1991**, *16* (4), 561.
(11) Kumar, D. *J. Polym. Sci., Polym. Chem. Ed.* **1970**, *18*, 1376.
(12) Sazanov, Yu. N.; Krasilnikova, L. V.; Shcherbakova, L. M. *Eur. Polym. J.* **1975**, *11*, 801.
(13) Bruck, S. D. *Polymer* **1965**, *6*, 49.
(14) Krasovskii, A. N., Antonov, N. P.; Koton, M. M.; Kalmin'sh, K. K.; Kudryavtsev, V. V. *Polym. Sci. USSR (Engl. Transl.)* **1979**, *21*, 1038.
(15) Kumar, D. *J. Polym. Sci., Polym. Chem. Ed.* **1980**, *18*, 1375.
(16) Baise, A. I. *J. Appl. Sci.* **1986**, *32*, 4043.
(17) Waldbauer, R. O.; Rogers, M. E.; Arnold, C. A.; York, G. A.; Kim, Y.; McGrath, J. E. *Polym. Prepr. (Am. Chem. Soc., Div. Polym. Chem.)* **1990**, *31* (2), 432.
(18) McGrath, J. E.; Rogers, M. E.; Arnold, C. A.; Kim, Y. J.; Hedrick, J. C. *Makromol. Chem., Macromol. Symp.* **1991**, *51*, 103.
(19) Rogers, M. E.; Woodard, H.; Brennan, A.; Cham, P. M.; Marand, H.; McGrath, J. E. *Polym. Prepr. (Am. Chem. Soc., Div. Polym. Chem.)* **1992**, *33* (1), 461.
(20) McGrath, J. E., Grubbs, H.; Rogers, M. E.; Gungor, A.; Joseph, W. A.; Mercier, R.; Rodrigues, D.; Wilkes, G. L.; Brennan, A. *Int. SAMPE Tech. Conf.* **1991**, *23*, 119.
(21) Arnold, C. A.; Summers, J. D.; Chen, Y. P.; Bott, R. H.; Chen, D.; McGrath, J. E. *Polymer* **1989**, *30*, 986.
(22) Wilkens, D. L.; Arnold, C. A.; Jurek, M. J.; Rogers, M. E.; McGrath, J. E. *J. Thermoplas. Compos. Mater.* **1990**, *3* (1), 4.
(23) Gungor, A.; Smith, C. D.; Wescott, J.; Srinivasan, S.; McGrath, J. E. *Polym. Prepr. (Am. Chem. Soc., Div. Polym. Chem.)* **1991**, *32* (1), 172; *J. Polym. Sci. Polym. Chem. Ed.*, in press.
(24) Rogers, M. E.; Rodrigues, D.; Wilkes, G. L.; McGrath, J. E. *Polym. Prepr. (Am. Chem. Soc., Div. Polym. Chem.)* **1991**, *32* (1), 176.
(25) Rogers, M. E.; Grubbs, H.; Brennan, A.; Rodrigues, D.; Lin, T.; Marand, H.; Wilkes, G. L.; McGrath, J. E. *Int. SAMPE Symp. Exhib.* **1992**, *37*, 717.
(26) McGrath, J. E.; Grubbs, H.; Rogers, M. E.; Mercier, R.; Joseph, W. A.; Alston, W.; Rodrigues, D.; Wilkes, G. L. *Sample Tech. Conf. Proc.* **1991**, *23*, 119.
(27) Ginsberg, R.; Susko, J. R. In *Polyimides: Synthesis, Characterization, and Applications*, Mittal, K. L., Ed.; Plenum: New York, 1984; Vol. 1. p 237.
(28) Frayer, P. D. In *Polyimides: Synthesis, Characterization, and Applications*; Mittal, K. L., Ed.; Plenum: New York, 1984; Vol. 1, p 273.
(29) Laius, L. A.; Bessonov, M. I.; Florinskii, F. S. *Polym. Sci. USSR (Engl. Transl.)* **1971**, *13*, 2257.
(30) St. Clair, A. K.; St. Clair, T. L. *Polym. Prepr. (Am. Chem. Soc., Div. Polym. Chem.)* **1986**, *27* (2), 406.
(31) Young, P. R.; Chang, A. C. *SAMPE J.* **1986**, *22*, 70.
(32) Lavrov, S. V.; Kardash, I. Ye.; Pravednikov, A. N. *Polym. Sci. USSR (Engl. Transl.)* **1977**, *10*, 2727.
(33) Bessonov, M. I.; Koton, M. M.; Kudryavtsev, V. V.; Laius, L. A. *Polyimides: Thermally Stable Polymers*, 2nd ed.; Plenum: New York, 1987; pp 14–56.
(34) Chu, N. J.; Huang, J. W.; Chang, C. H. *Makromol. Chem.* **1989**, *190*, 1799.
(35) Kruez, J. A.; Endrey, A. L.; Gay, F. P.; Sroog, C. E. *J. Polym. Sci., Part A-1* **1966**, 2607.
(36) Chu, Ning-Jo; Huang, Jian-Wen. *Polym. J.* **1990**, *22*, 725.
(37) Pyun, E.; Mathisen, R. J.; Sung, C. S. P. *Macromolecules* **1989**, *22*, 1174.
(38) Laius, L. A.; Bessonov, M. I.; Kallistova, Ye. V.; Adrova, N. A.; Florinskii, F. S. *Polym. Sci. USSR* **1967**, *9*, 2470.
(39) Lavrov, S. V.; Arsashnikov, A. Ya.; Kardash, I. Ye.; Pravednikov, A. N. *Polym. Sci. USSR (Engl. Transl.)* **1977**, *19*, 1212.
(40) Lavrov, S. V.; Talankina, O. B.; Vorob'ev, V. D.; Izumnikov, A. L.; Kardash, I. E.; Pravednikov, A. N. *Polym. Sci. USSR (Engl. Transl.)* **1980**, *22*, 2069.
(41) Brekner, M. J.; Feger, C. *J. Polym. Sci., Part A* **1987**, *25*, 2005.
(42) Numata, Shun-Ichi; Fujisaki, Koji; Kinjo, N. In *Polyimides: Synthesis, Characterization, and Applications*, Mittal, K. L., Ed.; Plenum: New York, 1984; Vol. 1, p 259.
(43) Laius, L. A.; Tsapovetskii, M. I. In *Polyimides: Synthesis and Characterization*, Mittal, K. L., Ed.; Plenum: New York, 1984; Vol. 1, pp 295–309.
(44) Milevskaya, I. S.; Lukasheva, N. V.; El'yashevich, A. M. *Polym. Sci.* USSR (*Engl. Transl.*) **1979**, *21*, 1427.
(45) Kruez, J. A.; Endrey, A. L.; Gay, F. P.; Sroog, C. E. *J. Polym. Sci., Part A-1* **1966**, 2607.
(46) Denisov, V. M.; Kol'tsov, A. I.; Mikhailova, N. V.; Nikitin, V. N.; Bessonov, M. I.; Glukhov, N. A.; Shcherbakova, L. M. *Polym. Sci. USSR (Engl. Transl.)* **1976**, *18*, 1780.
(47) Nechayev, P. P.; Vygodskii, Ya. S.; Zaikov, G. Ye.; Vinogradova, S. V. *Polym. Sci. USSR (Engl. Transl.)* **1976**, *18*, 1903.
(48) Kamzolkina, Ye. V.; Teiyes, G.; Nechayev, P. P.; Gerashchenko, Z. V.; Vygodskii, Ya. S.; Zaikov, G. Ye. *Polym. Sci. USSR (Engl. Transl.)* **1976**, *18*, 3161.

(49) Bell, V. L.; Stump, B. L.; Gager, H. *J. Polym. Sci. Polym. Chem. Ed.* **1976**, *14*, 2275.
(50) Cotts, P. M.; Volksen, W.; Ferline, S. *J. Polym. Sci., Part B* **1992**, *30*, 373.
(51) Young, P. R.; Chang, A. C. *SAMPE J.* **1986**, March/April, 70.
(52) Young, P. R.; Davis, J. R. J.; Chang, A. C.; Richardson, J. N. *J. Polym. Sci., Polym. Chem. Ed.* **1990**, *28*, 3107.
(53) Sacher, E. *J. Macromol. Sci. Phys.* **1986**, *B25*, 405.
(54) Snyder, R. W.; Thomson, B.; Bartges, B.; Czerniawski, D.; Painter, P. C. *Macromolecules* **1989**, *22*, 4166.
(55) Kuroda, S.; Terauchi, K.; Nogami, K.; Mita, I. *Eur. Polym. J.* **1989**, *25*, 1.
(56) Kuroda, S. I.; Mita, I. *Eur. Polym. J.* **1989**, *25*, 611.
(57) Dine-Hart, R. A.; Parker, D. B. V.; Wright, W. W. *Br. Polym. J.* **1971**, *3*, 222.
(58) Dine-Hart, R. A.; Parker, D. B. V.; Wright, W. W. *Br. Polym. J.* **1971**, *3*, 226.
(59) Tsapovetskii, M. I.; Laius, L. A.; Zhukova; Shibayev, L. A.; Stepanov, N. G.; Bessonov, M. I.; Koton, M. M. *Polym. Sci. USSR* (*Engl. Transl.*) **1988**, *30*, 295.
(60) Koton, M. M.; et al. In *Polyimides: Materials, Chemistry and Characterization*; Feger, C. J., Khojasteh, M. M., McGrath, J. E., Eds.; Elsevier Science Publishers BV: Amsterdam, 1989; p 403.
(61) Koton, M. M.; Frenkel's, S. Ya.; Panov, Yu. N.; Bolotnikova, L. S.; Svetlichnyi, V. M.; Shibayev, L. A.; Kulichikhin, S. G.; Krupnova, Ye. Ye.; Reutov, A. S.; Ushakova, I. L. *Poly. Sci. USSR* (*Engl. Transl.*) **1988**, *30*, 2600.
(62) Dine-Hart, R. A.; Wright, W. W. *J. Appl. Polym. Sci.* **1967**, *11*, 609.
(63) Bower, G. M.; Frost, L. W. *J. Polym. Sci., Part A* **1963**, *1*, 3135.
(64) Cotts, P. M. In *Polyimides: Synthesis, Characterization and Applications*; Mittal, K. L., Ed.; Plenum: New York, 1984; Vol. 1, p 223.
(65) Wallach, M. L. *J. Polym. Sci., Part A-2* **1967**, *5*, 653.
(66) Marie-Florence Grenier-Loustalot; Joubert, F.; Grenier, P. *J. Polym. Sci., Polym. Chem. Ed.* **1991**, *29*, 1649.
(67) Matsuura, T.; Hasuda, Y.; Nishi, S.; Yamada, N. *Macromolecules* **1991**, *24*, 5001.
(68) Korshak, V. V.; Urman, Ya. G.; Alekseeva, S. G.; Slonim, I. Ya.; Vinogradova, S. V.; Vygodskii, Ya. S.; Nagiev, Z. M. *Makromol. Chem., Rapid Commun.* **1984**, *5*, 695.
(69) Navarre, M. In *Polyimides: Synthesis, Characterization, and Applications*; Mittal, K. L., Ed.; Plenum: New York, 1984; Vol. 1, pp 429–442.
(70) Pryde, C. A. *J. Polym. Sci.* **1989**, *A27*, 711.
(71) Harris, D. C. *Quantitative Chemical Analysis*, Freeman, W. H. & Co.: New York, 1980; p 372.
(72) Espenson, J. H. *Chemical Kinetics and Reaction Mechanism*; McGraw-Hill Book Co.: New York, 1981; p 34.
(73) Moore, J. W.; Pearson, R. G. *Kinetics and Mechanism*, 3rd ed.; John Wiley & Sons, Inc., United Publishing & Promotion Co., Ltd.: New York, 1984; p 60.
(74) Serchenkova, S. V.; Shablygin, M. V.; Kravchenko, T. V.; Oprits, Z. G.; Kudryavtsev, G. I. *Polym. Sci. USSR* (*Engl. Transl.*) **1978**, *20*, 1284.
(75) Korzhavin, L. N.; Shibayev, L. A.; Bronnikov, S. V.; Antonov, T. A.; Sazanov, Yu. N.; Frenkel', S. Ya. *Polym. Sci. USSR* (*Engl. Transl.*) **1980**, *22*, 2220.
(76) Lavrov, S. V.; Kardash, I. Ye.; Pravednikov, A. N. *Polym. Sci. USSR* (*Engl. Transl.*) **1977**, *19*, 2727.
(77) Snyder, R. W. In *Polyimides: Materials, Chemistry, and Characterization*, Feger, C. J., Khojasteh, M. M., McGrath, J. E., Eds.; Elsevier Science Publishers BV: Amsterdam, 1989; p 363.
(78) Pravednikov, A. N.; Kardash, I. Ye.; Glukhoyedov, N. P., Ardashnikov, A. Ya. *Polym. Sci. USSR* (*Engl. Transl.*) **1973**, *15*, 399.
(79) Kardash, I. Ye.; Ardashnikov, A. Ya.; Yakubovich, V. S.; Braz, G. I.; Yakubovich, A. Ya.; Pravednikov, A. N. *Polym. Sci. USSR* (*Engl. Transl.*) **1967**, *9*, 2160.
(80) Espenson, J. H. *Chemical Kinetics and Reaction Mechanism*; McGraw-Hill Book Co.: New York, 1981; p 120.
(81) Lyon, K. R.; McGrath, J. E. *SAMPE* **1991**, *36*, 417.
(82) Lyon, K. R.; McGrath, J. E.; Geibel, J. F. *Polym. Mater. Sci. Eng.* **1991**, *65*, 249.
(83) Pine, S. H.; Hendrickson, J. B.; Cram, D. J.; Hammond, G. S. *Organic Chemistry*; McGraw-Hill, Kogakusha, Ltd.: Tokyo, 1980; p 286.
(84) Lowry, T. H.; Richardson, K. S. *Mechanism and Theory in Organic Chemistry*, 2nd ed., 1981; pp 185, 635–641.